Inhibition of the MRP1-mediated transport of the menadione-glutathione conjugate (thiodione) in HeLa cells as studied by SECM

Dipankar Koley and Allen J. Bard[1]

Center for Electrochemistry, Department of Chemistry and Biochemistry, University of Texas at Austin, 1 University Station A5300, Austin, TX 78712-0165

Edited by Royce W. Murray, University of North Carolina, Chapel Hill, NC, and approved April 24, 2012 (received for review February 16, 2012)

Oxidative stress induced in live HeLa cells by menadione (2-methyl-1,4-napthaquinone) was studied in real time by scanning electrochemical microscopy (SECM). The hydrophobic molecule menadione diffuses through a living cell membrane where it is toxic to the cell. However, in the cell it is conjugated with glutathione to form thiodione. Thiodione is then recognized and transported across the cell membrane via the ATP-driven MRP1 pump. In the extracellular environment, thiodione was detected by the SECM tip at levels of 140, 70, and 35 μM upon exposure of the cells to menadione concentrations of 500, 250, and 125 μM, respectively. With the aid of finite element modeling, the kinetics of thiodione transport was determined to be 1.6×10^{-7} m/s, about 10 times faster than menadione uptake. Selective inhibition of these MRP1 pumps inside live HeLa cells by MK571 produced a lower thiodione concentration of 50 μM in presence of 500 μM menadione and 50 μM MK571. A similar reduced (50% drop) thiodione efflux was observed in the presence of monoclonal antibody QCRL-4, a selective blocking agent of the MRP1 pumps. The reduced thiodione flux confirmed that thiodione was transported by MRP1, and that glutathione is an essential substrate for MRP1-mediated transport. This finding demonstrates the usefulness of SECM in quantitative studies of MRP1 inhibitors and suggests that monoclonal antibodies can be a useful tool in inhibiting the transport of these MDR pumps, and thereby aiding in overcoming multidrug resistance.

Multidrug resistance (MDR) pumps play a critical role in the detoxification pathway and cell survival under the oxidative stress caused by quinone or quinone-based chemotherapeutic drugs. Among the MDR pumps, the multidrug resistance protein (MRP1) pump is known to pump a broad variety of organic anions out of cells (1). According to the accepted model, MRP1 pumps out glutathione-S-conjugates (GS-conjugates), oxidized glutathione (GSSH), and reduced glutathione (GSH) as well as the unmodified drugs in the presence of physiological concentration of GSH; for example vincristine or daunorubicin are transported out of the cells by MRP1 in unmodified form in the presence of GSH (2). The cytotoxicity of a particular drug also depends on the types of MDR pumps and whether they are overexpressed in a cell under oxidative stress. For example, MRP pumps are known to be highly expressed in colon, breast and ovarian cancer cells whereas P-glycoprotein (Pgp) pumps are widely expressed in colon, renal and liver cancer cells but poorly expressed in breast, lung, and ovarian tumors (3). Hence, there are differences between the oxidative stress response of one type of cell to another and this is significant when comparing the effects of xenobiotics being added to different cells. In rat platelets, 85% intracellular GSH was reported to deplete as menadione-GSH conjugate, whereas in hepatocytes, 75% of intracellular GSH was depleted by menadione due to formation of GSSG (4).

Depending on their modifications, quinones induce cytotoxicity in living cells by different pathways (4). A recycler such as 2,3-dimethoxy-1,4-napthaquinone exhibits oxidative stress purely by redox cycling, forming semiquinones, superoxide and hydroxyl radicals; thus depleting the reduced glutathione or GSH pool present inside the cell by forming oxidized glutathione or GSSH. A second type of quinone, an arylator such as 1,4-benzoquinone, exhibits cytotoxicity through arylation, forming GS-conjugates and thus depleting the intracellular GSH. Quinone-based oxidative stress in living cells differs from oxidative stress based on extracellularly administered hydrogen peroxide. The later agent is capable of inducing lipid peroxidation and subsequently rupturing the cell membrane before even entering the cell. Other types of quinone such as menadione (2-methoxy-1,4-napthaquinone) can act as both a redox cycler and arylator. Because of its hydrophobicity, menadione can pass through an intact cell membrane and induce oxidative stress by producing superoxide and hydroxyl radical. As part of the cells defense against such oxidative stress, GSH present inside the cell subsequently undergoes sacrificial nucleophilic addition or arylation with menadione in presence of the GS-transferase enzyme, forming menadione-S-glutathione (thiodione). However, the conjugate retains the ability to carry out redox recycling to form superoxide and hydroxyl radical, and this is not, by itself, an effective detoxification pathway unless the thiodione has been recognized by GS-X or MDR pumps as a substrate and pumped out of the cell by an ATP-driven process (Fig. 1) (5–10).

MRP1 transports both endogenous substrates such as glutathione, steroids, LTC_4, LTD_4, LTE_4 as well as substrates like doxorubicin, daunorubicin, GS-conjugates, and vinblastine. However, LTC_4 has the highest affinity for MRP1 (2, 6, 9, 11–15). The inhibition of these MRP1 pumps increases the accumulation of intracellular xenobiotics or their conjugates; which therefore increases the cytotoxicity of the drugs towards the cell. MK571 (5-(3-(2-(7-chloroquinolin-2-yl) ethenyl) phenyl)-8-dimethylcarbamyl-4,6-dithiaoctanoic acid), an LTD_4 receptor antagonist, has been reported to act as competitive inhibitor for MRP1-mediated transport, both for GS-conjugate transport (such as thiodione) as well as for the transport of unconjugated GSH-mediated xenobiotics, such as daunorubicin (15–26).

To understand mechanistically the function of this MRP1 pump in physiological condition, several immunoblot, immunoprecipitate and immunofluorescence based studies (27–35) have been made with MRP1-specific antibodies such as QCRL-1, QCRL-2, QCRL-3, QCRL-4, and QCRL-6. These IgG class antibodies have been developed to recognize a specific sequence of amino acids in the MRP proteins. For example, QCRL-1,-2,-3 recognize 918–924, 617–858, 617–932 amino acid sequences respectively; whereas QCRL-4 and QCRL-6 bind overlapping sequences of 1294–1531 amino acids, -COOH proximal nucleotide binding site (NBD2). Hipfner and coworkers (27–30) have

Author contributions: D.K. and A.J.B. designed research; D.K. performed research; D.K. and A.J.B. analyzed data; and D.K. and A.J.B. wrote the paper.

The authors declare no conflict of interest.

This article is a PNAS Direct Submission.

[1]To whom correspondence should be addressed. Email: ajbard@mail.utexas.edu.

This article contains supporting information online at www.pnas.org/lookup/suppl/doi:10.1073/pnas.1201555109/-/DCSupplemental.

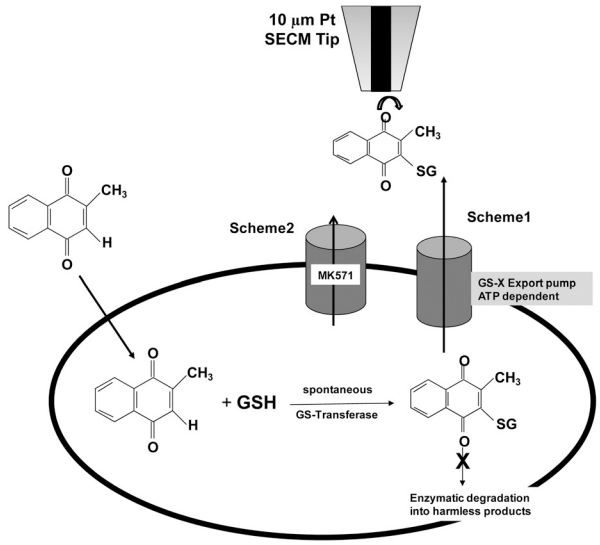

Fig. 1. Schematic diagram of cellular response to menadione in the presence or absence of MRP1 blocker MK571.

used these antibodies to map the topology of this entire transmembrane protein. An inhibitory effect of this antibody has also been reported with the endogenous substrate, LTC_4, whereas QCRL-3 has been reported (30, 35) to inhibit the photolabeling of MRP1 by LTC_4, proving that the 617–932 sequence is the major substrate binding site. Thus different kinds of antibodies can be used to understand the functionally important domain of the MRP1 pump, especially in terms of binding sites of different xenobiotic substrates and pumping out by an ATP-driven process.

Although there have been numerous studies on oxidative stress with different arrays of drugs and xenobiotics on diverse mammalian cell lines, most of them have been done with assays developed on lyzed cells after they were exposed to xenobiotics. Very few quantitative studies have been performed using live intact cells and their response in presence of xenobiotics, and fewer, particularly in terms of determining how transmembrane flux is affected by various antibodies that recognize different epitopes. Most of the immunoblot-based studies with antibodies and MDR pumps used antibodies to detect the pumps qualitatively, but very few studies have been done to demonstrate the blocking of a MRP1 pump efflux with an antibody in the dynamic environment of a live intact cell.

In previous studies (36, 37), we studied this process in yeast and heptablastoma cells with the SECM. In this paper we show that HeLa cells exposed to menadione form the GS-conjugate, which is then pumped into the extracellular environment by ATP-driven MDR pumps. The quantitative estimation of thiodione flux out of the living cells was measured by SECM on a real time basis. The selective blocking by MK571 of these MRP1 pumps present in a live HeLa cell was also demonstrated; thus confirming that thiodione is indeed a substrate for MRP1 pumps and plays an important role in the cellular defense mechanism against quinone-based oxidative stress. In addition, a monoclonal antibody such as QCRL-4 was able to inhibit the thiodione flux under oxidative stress, again demonstrating the relevant function of MRP1.

Results

Cytotoxicity Experiments. Cell viability tests showed that in the presence of 500 μM menadione (*SI Appendix*, Fig. S1) less than 40% of the cells were alive after 3 h; whereas viability was unaffected during a 60 min period. Hence all SECM experiments were performed within a 60 min time frame. Based on a viability assay (*SI Appendix*, Fig. S2) the HeLa cells maintained membrane integrity for 30 min after addition of 50 μM MK571 and 500 μM menadione. Hence, the cells were incubated for 60 min in 50 μM MK571 solution before replacing the solution with a suitable MK571 and menadione mixture for SECM experiments.

Thiodione Flux from a Monolayer of HeLa Cells. The cellular response for different concentrations of menadione (500, 250, 125 μM) with time (min) is shown in Fig. 2*B*. The thiodione concentration was detected with a 10 μm Pt tip at a distance of about 90 μm from the cellular monolayer. The concentration was calculated from the cyclic voltammetry recorded at approximately one-minute intervals as shown in *SI Appendix*, Fig. S3. The current at +0.4 V was converted into concentration using the equation $i_{ss} = 4nFaDC^*$, where a is the radius of the electrode, D is the diffusion coefficient, and C^* is the concentration. A gradual increase of thiodione concentration was recorded for 20 min after addition of 500 μM menadione, after which the concentration reached a quasi steady state of 140 μM (Fig. 2*B*). Quasi steady state thiodione concentrations of 70 μM and 35 μM were also recorded for 250 μM and 100 μM menadione additions, respectively. Assuming a constant flux of thiodione through the cellular monolayer at quasi steady state, the number of molecules pumped out of the cells on exposure of 500 μM of menadione was calculated to be 2.6×10^{-17} mol/cell/s or 16×10^6 molecules/cell/s.

Though care has been taken (using a vibration free stage) to measure the development of thiodione concentration above the cells w.r.t. time, there is a possibility that natural convection might set in as the experiments are performed for 30 min duration. However, the effect of such natural convection is somewhat minimized with the use of 10 μm diameter UME as an SECM tip. In addition, the variability of biological samples probably supersede the small error due to effect of natural convection. Future experiments, however, could investigate this under idealized electrochemical condition.

Model of Thiodione Release. Fig. 2*B* shows the fitting of experimental (points expressed in various symbols) and simulated response (solid lines) for a monolayer of HeLa cells in the presence of 500, 250, and 125 μM menadione. The kinetics of menadione uptake was 1.6×10^{-8} m/s, and rate of thiodione pumping out was calculated to be 1.6×10^{-7} m/s. The rate constant for the homogenous reaction between menadione and glutathione was adjusted to be between 4 to 10 s^{-1} and that of the intracellular glutathione concentration between 20 to 5 mol/m^3 for varying concentrations of menadione exposure. The simulation parameters were determined using 60 min (short-time) simulations. The comparison of simulation and experiment for longer time (160 min) SECM of 500 μM menadione response is shown in Fig. 2*D*. Except for the duration, all simulation parameters were the same as the short-time simulation.

Inhibition of MRP1 Pump by MK571. Fig. 3 shows the thiodione efflux from a monolayer of cells in the absence and presence of different concentrations of MK571, an LTD_4 receptor antagonist and a notable MRP1 inhibitor. The thiodione concentration was 50 μM ± 10 μM in presence of 50 μM MK571 and 500 μM menadione. Error bars were calculated from three separate experiments. The cells were incubated in 50 μM MK571 for 60 min before adding any menadione-MK571 solution. The control experiment was done following the same protocol except without any menadione in the solution.

Inhibition of MRP1 Pump by QCRL-4 Antibody. Fig. 4 shows the normalized thiodione concentration vs. time in the absence (upper line) and presence (lower line) of QCRL-4 antibody. The effluxed thiodione concentration showed a drop of 50% when transfected with QCRL-4 antibodies. The thiodione concentration was normalized against the average thiodione concentration produced using the same set of experiments in the presence of

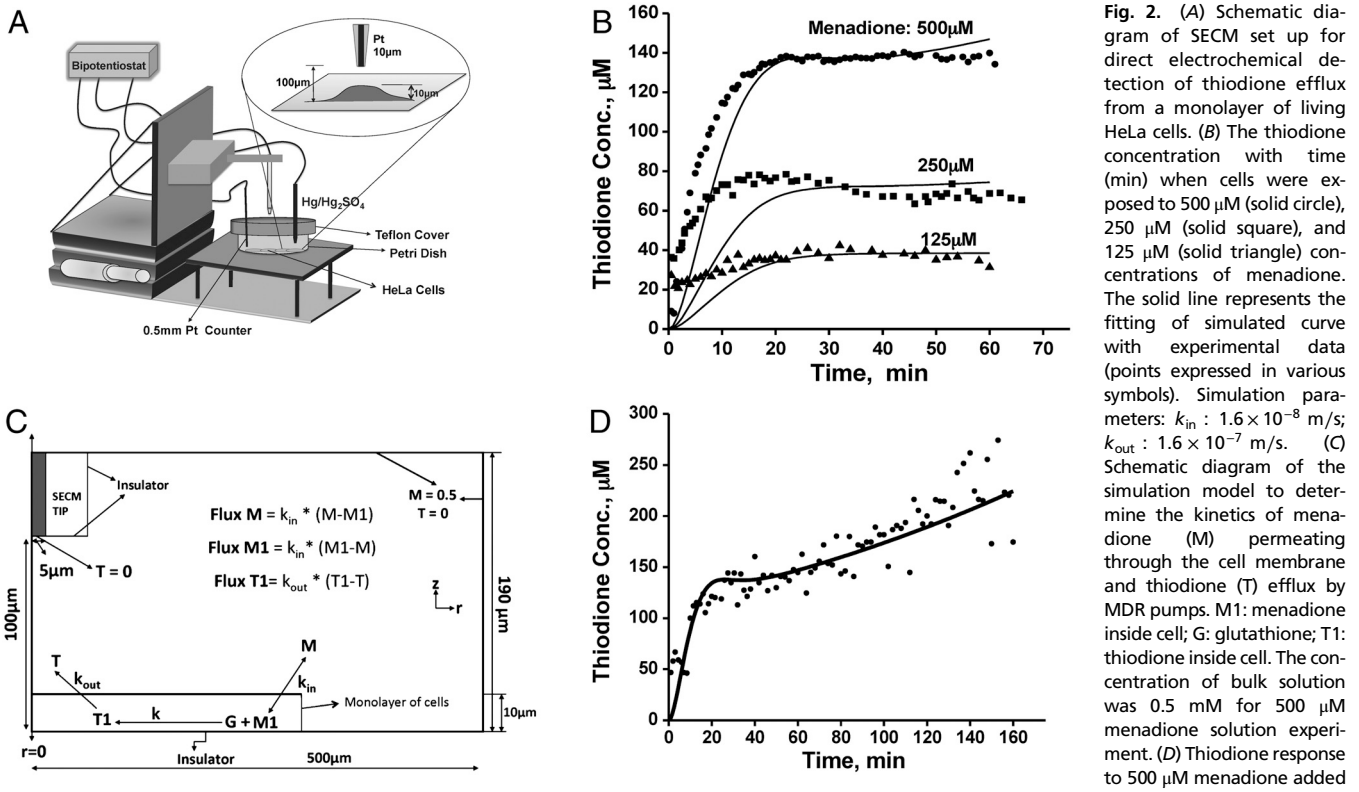

Fig. 2. (*A*) Schematic diagram of SECM set up for direct electrochemical detection of thiodione efflux from a monolayer of living HeLa cells. (*B*) The thiodione concentration with time (min) when cells were exposed to 500 μM (solid circle), 250 μM (solid square), and 125 μM (solid triangle) concentrations of menadione. The solid line represents the fitting of simulated curve with experimental data (points expressed in various symbols). Simulation parameters: k_{in} : 1.6×10^{-8} m/s; k_{out} : 1.6×10^{-7} m/s. (*C*) Schematic diagram of the simulation model to determine the kinetics of menadione (M) permeating through the cell membrane and thiodione (T) efflux by MDR pumps. M1: menadione inside cell; G: glutathione; T1: thiodione inside cell. The concentration of bulk solution was 0.5 mM for 500 μM menadione solution experiment. (*D*) Thiodione response to 500 μM menadione added to HeLa cells for 160 min (solid circle points). Solid line represents the simulated curve.

500 μM menadione without any blocker. The thiodione concentration was normalized because of the variation of thiodione efflux from one set of experiments to another. The thiodione concentration (μM) vs. time (min) plots for four sets of independent experiments are given in the *SI Appendix*, Fig. S5. In all four experiments in the *SI Appendix*, Fig. S5 *A–D*, the thiodione concentration dropped on the average from 100 ± 10 μM to 50 ± 10 μM after the cells were transfected with QCRL-4 antibodies. Error bars were calculated from four separate experiments. A fluorescence-based viability test was also performed with transfected HeLa cells by adding 500 μM menadione. No additional loss in cell viability was observed beyond that observed due to addition of 500 μM menadione alone to nontransfected HeLa cells (*SI Appendix*, Fig. S1).

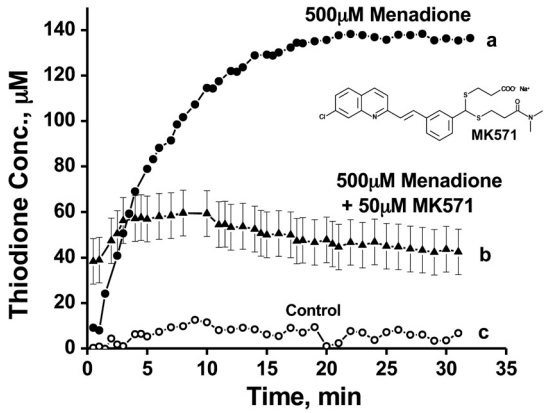

Fig. 3. (*A*) The thiodione efflux from a monolayer of HeLa cells in the absence of MRP1 blocker MK571. (*B*) Thiodione concentration in the presence of 50 μM of MK571 and 500 μM menadione. (*C*) Control experiment in the presence of MK571 blocker. All the experimental conditions were the same except the control current was recorded without any menadione in the solution.

Discussion

Cellular Response to Menadione Induced Oxidative Stress. Quantitative detection of thiodione efflux (Fig. 2*B*) due to the addition of menadione to HeLa cells confirmed the schematic model proposed in Fig. 1. Menadione, an arylator and redox cycling molecule, can induce oxidative stress in HeLa cells by forming reactive oxygen species. To protect itself from such oxidative stress, the cell maintains a pool of GSH in mM concentration. When the hydrophobic molecule menadione enters a live cell, it oxidizes the GSH and also forms GS-conjugates, thiodione, in the presence of the GST enzyme. This causes a disruption in the GSH/GSSG ratio as well as depletion of GSH. Thiodione formed inside the cell is recognized by the transmembrane MRP1 pump by its glutathione moiety and transported out of HeLa cells in an ATP-driven process. The extracellular thiodione in solution is then detected by an SECM tip located 90 μm away from the cells. Fig. 2*B* shows such a cellular response upon exposure to different concentrations of menadione and the resulting build up of the thiodione concentration over the cellular monolayer in the extracellular environment. The gradual increase in thiodione concentration and maintenance of a quasi steady state for 60 min also confirms that the thiodione is transported out of a cell in a controlled ATP-driven process instead of diffusing out of a leaking cell membrane. The cell is able to survive from oxidative stress for 60 min in the presence of 500 μM menadione. In addition, the viability and existence of intact cell membranes of the HeLa cells is supported by an independent test of viability based on cell membrane integrity (*SI Appendix*, Fig. S1).

The detection of the varying concentration of thiodione (Fig. 2*B*) outside cells suggests that thiodione transport is not only a controlled, ATP-driven, MDR-mediated process, but also

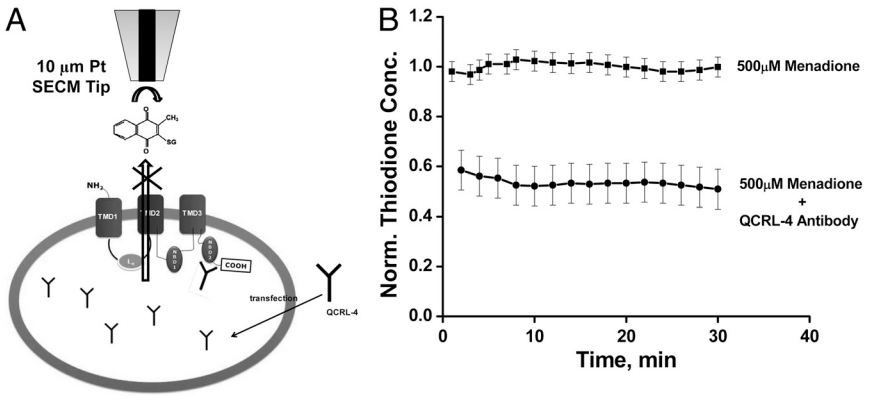

Fig. 4. (*A*) Schematic diagram (not to scale) of transfection of QCRL-4 monoclonal antibody and subsequent binding to NBD2 domain of MRP1 pump. (*B*) Normalized thiodione concentration in presence of 500 μM menadione (upper line) without and (lower line) with antibody QCRL-4. Thiodione concentration is normalized against the average thiodione concentration produced in each individual experiment without any blocker antibody. Tip was positioned at 80 μm distance from petri dish to record the thiodione efflux.

that a live cell is able to up-regulate and down-regulate thiodione transport as necessary. The cell is able to regulate transport by recruiting more MDR proteins (produced from golgi) in its membrane, as well as modulating its GSH-producing enzyme, (24) which may contribute to increased thiodione flux.

As shown in Fig. 2*B*, thiodione has been effluxed to a concentration of 140 μM upon addition of 500 μM menadione, which is only 28% of the menadione concentration exposed. A similar response was observed for 250 and 125 μM menadione exposure. In general the menadione concentration outside the cell should ultimately reach near the intracellular menadione concentration, which should lead to a higher thiodione concentration than that measured. Such a contrast has been reported before by our group (36, 37) for menadione transport with yeast and hepatoblastoma cell lines. For liver cancer cells the thiodione efflux recorded to be 100% of menadione exposed, whereas for yeast it is only reported to be 10% of the menadione exposed. This contrast may be due to the way a particular cell functions.

The thiodione molecule produced inside the cell enzymatically also retains the recycling property and has the ability to produce more superoxide or hydroxyl radical, and thus prove toxic to the cell. Therefore, any accumulated thiodione, in addition to any menadione present inside the cell, can also contribute to lipid peroxidation. A living cell can only survive under such a stressed condition if it can keep up with the rate of production of sacrificial GSH by pumping out thiodione. This may explain why the cell viability dropped from 70% to below 40% (viability assay) during a 2 to 3 h time period as well as from a long time (60 min) SECM experiment. Fig. 2*D* shows further the monotonic rise of thiodione concentration outside the cell monolayer until 240 min after reaching a quasi steady state at 60 min. This could be taken as the beginning of uncontrolled leaking of thiodione outside the cell due to lipid peroxidation of cellular membrane. In addition, the trypan blue viability assay also confirms the rupture of cell membrane after 120 min with the addition of 500 μM menadione.

Model of Thiodione Efflux from a Monolayer of HeLa Cells. To elucidate the processes occurring inside the cell, a mathematical model was developed to represent the kinetics of menadione uptake and thiodione pumping out of cells (Fig. 2*C*). The simulated fitted thiodione response curve (solid line) with respect to time (min) is shown in Fig. 2*B* for 500, 250, and 125 μM menadione concentration exposure. The calculated rate constant of thiodione transport is 1.6×10^{-7} m/s, 10 times faster than menadione uptake. The higher value of thiodione transport may represent an ATP-driven detoxification pathway; in contrast to menadione uptake which is solely driven by diffusion by the concentration gradient across the cell membrane. A similar rate of thiodione pumping larger than menadione influx was found in earlier studies with yeast and heptablastoma cells (36, 37).

Fig. 2*D* shows the simulated fitting (solid line) of the gradual increase in thiodione concentration during a 160 min time interval due to the addition of 500 μM menadione to HeLa cells. Such a thiodione response was explained in the previous section as leaking due to collapse of a cellular membrane. In the simulation it is represented by an uncontrolled increase of thiodione above the cells.

Selective Blocking of MRP1 by MK571. Fig. 3 shows a significant drop in thiodione efflux concentration from 140 μM to 50 μM± 10 μM in the presence of 50 μM MK571 along with 500 μM menadione. This drop in thiodione efflux was not due to dead cells as an independent viability assay (*SI Appendix*, Fig. S2) shows 90% of the cells were alive during an experimental period of 30 min. The viability assay also shows that MK571 by itself is toxic to the cell and does affect the cell membrane integrity. However, the cell membrane permeability does change due to weak surfactant property of MK571. As a result, the rate of rise of thiodione flux (as seen in Fig. 3) may be affected; since the menadione diffusion inside the cell is the rate-limiting step. When the cells were incubated with 50 μM MK571, it could permeate through the cell membrane and enter the cell cytoplasma, affecting the Golgi body for producing and recruiting transmembrane proteins to the cell membrane. As mentioned above, the live cell undergoes rapid redistribution of transmembrane proteins or MRP pumps from the Golgi body to the cytoplasm to the plasma membrane upon exposure to low concentrations of xenobiotics. In other words, exposure to a low concentration of menadione up-regulates the MRP1 expression and stimulates GSH synthesis. But when cells are exposed to MK571, it prevents such early translocation of MRP1 proteins mostly localized in the Golgi (24). Hence the cell will have fewer pumps to transport thiodione outside of the cell, which in turn should contribute to less thiodione in the extracellular environment. In addition MK571, an LTD_4 receptor antagonist, also has the ability to competitively bind with the MRP1 inner leaflet drug binding site, decreasing the thiodione efflux. It can decrease both the flux of GSH as well as the drug efflux. The reduction in thiodione flux, demonstrates that thiodione is indeed pumped out of the cells by the MRP1 pumps.

Selective Blocking of MRP1 by QCRL-4 Antibody. As shown in Fig. 4 and *SI Appendix*, Fig. S5, the QCRL-4 antibody can be used to selectively block the MRP1 pump in a live intact HeLa cell. When delivered inside the cell, QCRL-4 has been shown to bind to the epitope 1294–1531 of the MRP1 protein, which is in proximity to the -COOH second nucleotide binding domain (NBD2) site. This

QCRL-4 antibody, once bound to the ATP binding site, prevents the MRP1 pump from changing its configuration, thus stopping any transport outside the cells. The specificity of QCRL-4 has been studied extensively by Cole and coworkers by immunoblotting and immunoprecipitation methods (30, 35) to show that this antibody selectively binds with the MRP1 protein sequence but not with any other protein such as Pgp. The monoclonal antibodies QCRL-2,-3,-4 have been shown to inhibit the transport of endogenous substrates such as LTC_4 and 17β-estradiol 17-(β-D-glucuronide) besides externally administered drugs such as daunorubicin and vincristine (13, 19, 32, 33). In these studies, complete or near complete inhibition of uptake of these substrates by the MRP-enriched inside out plasma membrane vesicles has been reported. However, in our study thiodione efflux dropped to produce a concentration of 100 ± 10 μM to 50 ± 10 μM from nontransfected to transfected live and intact HeLa cells. Here, such as difference is obvious as our study was done with live HeLa cells. To deliver the antibodies inside a live cell, one has to take into account the transfection efficiency of antibodies for a particular cell line. We assume in our case the transfection efficiency was about 50%. In addition, the live cell environment is dynamic and it can up-regulate and down-regulate MDR protein production when subjected to oxidative stress. In this study we have shown that if a sufficient amount of blocking antibodies are present inside the cells, the transporting functions of the MRP1 pumps can be impaired. This is confirmed with the 50% drop in thiodione efflux from transfected live HeLa cells in comparison to the nontransfected ones (Fig. 4). This is one of the few studies where the thiodione efflux has been quantitatively determined to be decreased, overcoming the multidrug resistance phenomenon in live cells in the presence of a xenobiotic such as menadione and monoclonal antibodies simultaneously.

Conclusions

When added to HeLa cells, menadione can permeate inside an intact cell due to its hydrophobic nature, and can induce oxidative stress. HeLa cells were observed to form GS-conjugates or thiodione in the presence of the GS-transferase. Thiodione was then recognized by MRP1 pumps due to its glutathione moiety, and subsequently pumped outside to the extracellular environment. This extracellular thiodione was then detected quantitatively in real time by an SECM tip positioned 90 μm above the cellular monolayer. The quasi steady state thiodione concentrations were 140, 70, and 35 μM after addition of 500, 250, and 125 μM menadione to the cells, respectively. Assuming a constant thiodione flux, approximately 16×10^6 molecules/s were calculated to be pumped out of a single cell on addition of 500 μM menadione. The cells were able to up-regulate or down-regulate their MRP1 pumps to modulate the thiodione efflux accordingly to the menadione exposure. In this study, MK571, a known MRP1 blocker, was used to demonstrate that MRP1 was the major carrier for thiodione transport in live HeLa cells. The extracellular thiodione concentration was shown to decrease to 40 ± 10 μM in presence of the class-I inhibitor, MK571. This confirmed that MRP1 pumps require the GSH moiety as a substrate to pump out any xenobiotics as a detoxification process. Additional experiments with MRP1-specific antibody QCRL-4 showed that it could selectively recognize the NBD2 binding site of MRP1; thus inhibiting the ATP-mediated thiodione efflux from live intact cells in the presence of menadione. Thiodione flux from transfected live HeLa cells was observed to drop by 50% from 100 ± 10 μM to 50 ± 10 μM in the presence of QCRL-4 monoclonal antibodies. This study henceforth can be extended to different antibodies capable of recognizing different epitopes of MRP1 in live intact cells. This would eventually help us to understand mechanistically the functions of these MDR pumps in live cells, pumping out different xenobiotics or chemotherapeutic agents. In the future, SECM can also be extended to identify any specific MDR pump for a particular xenobiotic transport used by a particular type of cell. It can also be used for rapid screening of different MRP1 blockers for a particular anti-cancer chemotherapeutic drug; and assist in designing pump inhibitors.

Materials and Methods

Chemicals. Menadione was purchased from Sigma Aldrich (M57405) and recrystallized from ethanol before use. All other chemicals were used as received. $MgSO_4$, $CaSO_4$ and K_2SO_4 were obtained from Fischer Scientific. D-glucose and Hepes were from Sigma-Aldrich. MK571 was obtained from Axxora (catalog number ALX-340-021) and QCRL-4 antibody (catalog number sc-18874) and Lipodin-Ab (catalog number 500115) from Santa Cruz Biotechnology and Abbiotec, respectively. All solutions were made with 18 MΩ Milli-Q (Millipore) reagent water treated with UV irradiation for 1 h.

Cell Culture. HeLa cells were purchased from ATCC (catalog number CCL-2) and cultured as per instructions provided by ATCC. Briefly, cells were grown and maintained in ATCC-formulated Eagle's Minimum Essential Medium (ATCC 30-2003) culture medium supplemented with 10% fetal bovine serum (ATCC 30-2020) on a tissue culture petri dish (Falcon 353801). The temperature was maintained at 37 °C in a water-jacketed incubator (model 2310, VWR Scientific) with 95% air and 5% CO_2. The cells were serum starved with 0.1% serum for 18–20 h inside the incubator before any SECM or cytotoxicity experiment.

When an appropriate cell coverage on the petri dish was obtained, the dish was taken out of the incubator, and the cells were washed with buffer solution (10 mM Hepes, 5.55 mM glucose, 75 mM Na_2SO_4, 1 mM $MgSO_4$ and 3 mM K_2SO_4) twice. The cells were then incubated with 1 mL of buffer solution at room temperature for 1 h. The buffer solution was later replaced by the appropriate experimental solution prepared with buffer.

Cytotoxicity Assay. We performed two types of cytotoxicity assays to determine the cell viability: trypan blue and fluorescent-based cytotoxicity assay. The detailed protocols about the corresponding assay tests are given in the *SI Appendix*. Note that separate cell viability tests in the presence of ferrocene methanol were performed and showed no change in the cell viability over the experimental time period.

SECM Experiment. A 10 μm diameter Pt ultramicroelectrode (UME) with RG 10 was used in SECM experiments. A detailed description of UME fabrication can be found elsewhere (38) Pt wire (0.5 mm) and Hg/Hg_2SO_4 were used as counter and reference electrodes, respectively. All the potentials given in this paper are vs. Hg/Hg_2SO_4.

A petri dish containing 80% coverage of HeLa cells was taken out of the incubator and placed on an SECM (Model 900B, CH Instruments) stage as shown in Fig. 2*A*. The cells were then washed twice with 1 mL of buffer solution and were subsequently incubated for 1 h in buffer-only solution. During the 1 h incubation period, an approach curve with oxygen as a mediator was performed to fix the tip-substrate (petri dish) distance at 90 μm, an optimum distance to record the rise of unique thiodione concentration profile. Buffer was then replaced by an appropriate concentration of menadione solution. Cyclic voltammograms (CV) were taken between −0.65 and +0.65 V at approximately every 1 min to clean the electrode surface as well as measure the concentration of thiodione being pumped out of the cellular monolayer attached to the dish. The basic electrochemistry of menadione, thiodione and glutathione has been described in an earlier publication (36, 37). Briefly, both menadione and thiodione reduce at 0.7 V, whereas thiodione shows a unique oxidation peak at 0.1 V. Glutathione is not electroactive in this potential range.

MK571 inhibition experiments. The petri dish with appropriate cell coverage was removed from the incubator and incubated on the SECM stage in buffer-only solution as described above. The cells were then further incubated for 1 h in 50 μM MK571 buffer solution, which were then replaced by 50 μM MK571 and 500 μM menadione solutions. The procedures thereafter were similar to those described above.

QCRL-4 antibody blocking experiments. The cells were cultured in a 1 cm diameter spot over a tissue-culture petri dish for 16 h inside the cell culture incubator as described in the Cell Culture section. The following antibody transfection procedure was performed for one dish only: 20 μL of antibody solution (4 μg) was mixed thoroughly with 4 μL Lipodin-Ab solution and incubated for 15 min at room temperature. 100 μL of medium-only (without serum) solution was added to the antibody/Lipodin-Ab solution, and then

immediately added to the cells. The cells were washed with 100 μL medium-only solution once before the antibody/Lipodin-Ab solution was added. The dish was then put back in the incubator for 5–6 h, then removed and washed twice with 400 μL of buffer. The dish was put on the SECM stage and incubated there for 1 h at room temperature. The buffer was replaced with 400 μL of 1 mM ferrocene methanol solution to perform an approach curve within 10–15 min. The tip-to-substrate distance was fixed at 90 μm. The cells were washed thrice with buffer solution after replacing the ferrocene methanol solution. A 500 μL drop of menadione solution was then added to the marked 1 cm spot of cells. Cyclic voltammograms were recorded between −0.65 and +0.65 V over 2 min intervals for 30 min.

Simulation Model. A schematic view of the simulation model is shown in Fig. 2*C*. The model was used to determine the kinetics of menadione uptake and thiodione release by a monolayer of living HeLa cells. We assumed the cells formed a perfect monolayer in the simulation model. The simulation was done in axial symmetry coordinates using Comsol Multiphysics software. The flux of menadione passing through the cell membrane was taken as $\pm k_{in} * (M\text{-}M1)$ where, M and $M1$ (mol/m^3) are the menadione concentrations outside and inside the cell; k_{in} (m/s) represents the surface rate constant of menadione uptake by live cells. The flux of menadione was considered in both directions between inside and outside the cell, because the movement of menadione molecules was taken as purely driven by the concentration gradient. Flux of thiodione through the cell membrane was considered as $k_{out} * (T1\text{-}T)$ where, $T1$ and T represent the thiodione concentrations inside and outside the cell; k_{out} represents rate of MDR-pump-mediated thiodione transport through cellular membrane. Here the flux was considered unidirectional, since the thiodione molecules were only pumped out of the cells by the ATP-driven MDR pumps. Initially there is no menadione present inside the cell, and the tip was held at a potential where the reaction, thiodione oxidation, was diffusion controlled at all times. More details about the Comsol Multiphysics model may be found in the *SI Appendix*.

1. Higgins CF (2007) Multiple molecular mechanism for multidrug resistance transporters. *Nature* 446:749–757.
2. Hooijberg JH, et al. (2000) The effect of glutathione on the ATPase activity of MRP 1 in its natural membranes. *FEBS Lett* 469:47–51.
3. Paul S, Breuninger LM, Tew KD, Shen H, Kruh GD (1996) ATP-dependent uptake of natural product cytotoxic drugs by membrane vesicles establishes MRP as a broad specificity transporter. *Proc Natl Acad Sci USA* 93:6929–6934.
4. Seung S, Lee JY, Lee MY, Park JS, Chung JH (1998) The relative importance of oxidative stress versus arylation in the mechanism of quinone-induced cytotoxicity to platelets. *Chem Biol Interact* 113:133–144.
5. Hultberg B, Anderson A, Isaksson A (1999) Thiol and redox reactive agents exert different effects on glutathione metabolism in HeLa cells culture. *Clin Chim Acta* 283:21–32.
6. Monks TJ, Lau SS (1997) Biological reactivity of polyphenolic-glutathione conjugates. *Chem Res Toxicol* 10:1296–1313.
7. Miller MG, Rodgers A, Cohen GM (1986) Mechanisms of toxicity of napthoquinones to isolated hepatocytes. *Biochem Pharmacol* 35:1177–1184.
8. Eaton DL, Bammler TK (1999) Concise review of the glutathione S-transferases and their significance to toxicology. *Toxicol Sci* 49:156–164.
9. Mueller CFH, et al. (2005) The role of multidrug resistance protein-1 in modulation of endothelial cell oxidative stress. *Circ Res* 97:637–644.
10. Roelofsen H, Hooiveld GJEJ, Koning H, Havinga R, Jansen PLM (1999) Glutathione S-conjugate transport in hepatocytes entering the cell cycle is preserved by a switch in expression from the apical MRP2 to the basolateral MRP1 transporting protein. *J Cell Sci* 112:1395–1404.
11. Zaman GJR, et al. (1995) Role of glutathione in the export of compounds from cells by the multidrug resistance-associated protein. *Proc Natl Acad Sci USA* 92:7690–7694.
12. Muller M, et al. (1994) Overexpression of the gene encoding the multidrug resistance-associated protein results in increased ATP-dependent glutathione S-conjugate transport. *Proc Natl Acad Sci USA* 91:13033–13037.
13. Renes J, Vries EGE, Nienhuis EF, Jansen PLM, Muller M (1999) ATP- and glutathione-dependent transport of chemotherapeutic drugs by the multidrug resistance protein MRP1. *Br J Pharmacol* 126:681–688.
14. Hipfner DR, Deeley RG, Cole SPC (1999) Structural, mechanistic and clinical aspects of MRP1. *Biochim Biophys Acta* 1461:359–376.
15. Jedlitschky G, et al. (1996) Transport of glutathione, glucuronate and sulfate conjugates by the MRP gene-encoded conjugate export pump. *Cancer Res* 56:988–994.
16. Leier I, et al. (1994) The MRP gene encodes an ATP-dependent export pump for Leukotriene C4 and structurally related conjugates. *J Biol Chem* 269:27807–27810.
17. Shen H, et al. (1996) Cellular and in vitro transport of glutathione conjugate by MRP. *Biochemistry* 35:5719–5725.
18. Karla PK, Pal D, Quinn T, Mitra AK (2007) Molecular evidence and functional expression of a novel drug efflux pump (ABCC2) in human corneal epithelium and rabbit cornea and its role in ocular drug efflux. *Int J Pharm* 336:12–21.
19. Tabas LB, Dantzig AH (2002) A high-throughput assay for measurement of multidrug resistance protein-mediated transport of leukotriene C4 into membrane vesicles. *Anal Biochem* 310:61–66.
20. Decory HH, Dumas KMP, Sheu SS, Federoff HJ, Anders MW (2001) Efflux of glutathione conjugate of monochlorobimane from striatal and cortical neurons. *Drug Metab Dispos* 29:1256–1262.
21. Tabas LB, Dantzig AH (2002) A high-throughput assay for measurement of multidrug resistance protein-mediated transport of leukotriene C4 into membrane vesicles. *Anal Biochem* 310:61–66.
22. Rigato I, Pascolo L, Fernetti C, Ostrow JJD, Tiribelli C (2004) The human multidrug-resistance-associated protein MRP1 mediates ATP-dependent transport of unconjugated bilirubin. *Biochem J* 383:335–341.
23. Gekeler V, Ise W, Sanders KH, Ulrich WR, Beck J (1995) The leukotriene LTD4 receptor antagonist MK571 specifically modulates MRP associated multidrug resistance. *Biochem Biophys Res Commun* 208:345–352.
24. Gennuso F, et al. (2004) Bilirubin protects astrocytes from its own toxicity by inducing up-regulation and translocation of multidrug resistance-associated protein 1 (Mrp1). *Proc Natl Acad Sci USA* 101:2470–2475.
25. Salerno M, Loechariyakul P, Saengkhae C, Suillerot AG (2004) Relation between the ability of some compounds to modulate the MRP1-mediated efflux of glutathione and to inhibit the MRP1-mediated efflux of daunorubicin. *Biochem Pharmacol* 68:2159–2165.
26. Jeong EJ, Jia X, Hu M (2005) Disposition of formononetin via enteric recycling: Metabolism and excreation in mouse intestinal perfusion and caco-2 cell models. *Mol Pharm* 2:319–328.
27. Hipfner DR, Gauldie SD, Deeley RG, Cole SPC (1994) Detection of the Mr 190,000 multidrug resistance protein, MRP, with monoclonal antibodies. *Cancer Res* 54:5788–5792.
28. Hipfner DR, Almquist KC, Stride BD, Deeley RG, Cole SPC (1996) Location of a protease-hypersensitive region in the multidrug resistance protein (MRP) by mapping of the epitope of MRP-specific monoclonal antibody QCRL-1. *Cancer Res* 56:3307–3314.
29. Hipfner DR, et al. (1999) Monoclonal antibodies that inhibit the transport function of the 190-kDa multidrug resistance protein, MRP. *J Biol Chem* 274:15420–15426.
30. Hipfner DR, Deeley RG, Cole SPC (1999) Structural mechanistic and clinical aspects of MRP1. *Biochim Biophys Acta* 1461:359–376.
31. Scheffer GL, et al. (2000) Specific detection of multidrug resistance proteins MRP1, MRP2, MRP3, MRP5, and MDR3 P-glycoprotein with a panel of monoclonal antibodies. *Cancer Res* 60:5269–5277.
32. Loe DW, Almquist KC, Deeley RG, Cole SPC (1996) Multidrug resistance protein (MRP)-mediated transport of leukotriene C4 and chemotherapeutic agents in membrane vesicles. *J Biol Chem* 271:9675–9682.
33. Loe DW, Deeley RG, Cole SPC (1998) Characterization of vincristine transport by the Mr 190,000 multidrug resistance protein (MRP): Evidence for cotransport with reduced glutathione. *Cancer Res* 58:5130–5136.
34. Hipfner DR, et al. (1998) Epitope mapping of monoclonal antibodies specific for the 190-kDa multidrug resistance protein (MRP). *Br J Cancer* 78:1134–1140.
35. Cole SPC, Deeley RG (1998) Multidrug resistance mediated by the ATP-binding cassette transporter protein MRP. *BioEssays* 20:931–940.
36. Mauzeroll J, Bard AJ (2004) Scanning electrochemical microscopy of menadione-glutathione conjugate export from yeast cells. *Proc Natl Acad Sci USA* 101:7862–7867.
37. Mauzeroll J, Bard AJ, Owhadian O, Monks TJ (2004) Menadione metabolism to thiodione in hepatoblastoma by scanning electrochemical microscopy. *Proc Natl Acad Sci USA* 101:17582–17587.
38. Bard AJ, Mirkin MV, eds. (2001) *Scanning Electrochemical Microscopy* (Marcel Dekker, New York) p 75.